OPEN

A highly-selective chloride microelectrode based on a mercuracarborand anion carrier

Marino DiFranco[1], Marbella Quinonez[1], Rafal M. Dziedzic[2], Alexander M. Spokoyny[2,3] & Stephen C. Cannon[1]*

The chloride gradient plays an important role in regulating cell volume, membrane potential, pH, secretion, and the reversal potential of inhibitory glycine and GABA$_A$ receptors. Measurement of intracellular chloride activity, a_{Cl}^i, using liquid membrane ion-selective microelectrodes (ISM), however, has been limited by the physiochemical properties of Cl$^-$ ionophores which have caused poor stability, drift, sluggish response times, and interference from other biologically relevant anions. Most importantly, intracellular HCO_3^- may be up to 4 times more abundant than Cl$^-$ (e.g. skeletal muscle) which places severe constraints on the required selectivity of a Cl$^-$ – sensing ISM. Previously, a sensitive and highly-selective Cl$^-$ sensor was developed in a polymeric membrane electrode using a trinuclear Hg(II) complex containing carborane-based ligands, [9]-mercuracarborand-3, or MC3 for short. Here, we have adapted the use of the MC3 anion carrier in a liquid membrane ion-selective microelectrode and show the MC3-ISM has a linear Nernstian response over a wide range of a_{Cl} (0.1 mM to 100 mM), is highly selective for Cl$^-$ over other biological anions or inhibitors of Cl$^-$ transport, and has a 10% to 90% settling time of 3 sec. Importantly, over the physiological range of a_{Cl} (1 mM to 100 mM) the potentiometric response of the MC3-ISM is insensitive to HCO_3^- or changes in pH. Finally, we demonstrate the biological application of an MC3-ISM by measuring intracellular a_{Cl}, and the response to an external Cl-free challenge, for an isolated skeletal muscle fiber.

Chloride ions (Cl$^-$) are the major inorganic free anions of the extracellular fluid, and together with organic bicarbonate ions (HCO$_3^-$) are the major intracellular anions[1,2]. The transmembrane Cl$^-$ gradient has a critical role in multiple cellular processes including cell volume regulation, acid-base homeostasis, fluid and electrolyte secretion, membrane excitability and the reversal potential of glycine and GABA$_A$-receptors at inhibitory synapses (see[1] and references therein). Moreover, the Cl$^-$ gradient is dynamic in many cells. For example, a developmental change in the expression of cation/chloride co-transporters reduces [Cl$^-$]$_i$ in mature neurons, and thereby converts GABA$_A$-receptor mediated responses from excitatory to inhibitory by shifting E_{Cl} to more negative potentials[3]. The steady-state Cl$^-$ gradient is determined by the balance of both passive transport, through ion channels as determined by the Cl$^-$ electrochemical potential, and by secondary active mechanisms via coupling to exchangers or cotransporters.

We sought a method to measure the Cl$^-$ gradient across the sarcolemma of skeletal muscle, where the resting potential (V_{rest}) is strongly dependent on the Cl$^-$ driving force, $V_m - E_{Cl}$, because these cells have a remarkably high resting chloride conductance ($g_{Cl} \sim 1$ mS/cm^2)[4,5]. Moreover, shifts of the sarcolemmal Cl$^-$ gradient have been causally implicated in attacks of periodic paralysis[6,7]. Understanding the roles of Cl$^-$ in muscle physiology, and all cells in general, demands knowing its concentration in the intra- and extracellular milieus, or more properly its activity (a_{Cl}) or "effective concentration", that ultimately determines the physiochemical reactivity of Cl$^-$ [8].

While measuring the extracellular a_{Cl}^o is relatively easy, non-destructive measurements of intracellular a_{Cl}^i poses major challenges. Basically, two methods are available to assess the intracellular chloride activity: (1) micro-photometric techniques, using either chemical or optogenetic Cl$^-$ sensors[9,10] and (2) potentiometric techniques with liquid membrane ion-selective microelectrodes (ISM for short)[11,12]. Photometric techniques allow for specific, high time resolution and space-resolved determination of changes in the activity of physiologically relevant ions, e.g. Ca^{2+}, Na$^+$, K$^+$, H$^+$, Cl$^-$. However, activity-dependent changes in optical properties of sensors are

[1]Department of Physiology, David Geffen School of Medicine at UCLA, Los Angeles, California, USA. [2]Department of Chemistry and Biochemistry, UCLA, Los Angeles, California, USA. [3]California NanoSystems Institute (CNSI), UCLA, Los Angeles, California, USA. *email: sccannon@mednet.ucla.edu

usually difficult to de-convolve into accurate molar units, and in some conditions, sensors can alter the extent and kinetics of the ion concentration changes aimed to be measured. Fluorescence life-time imaging circumvents some of these challenges[9], but requires specialized and expensive detection systems. In principle, an ISM is devoid of these limitations, and is expected to provide a direct determination of intracellular activity. In fact, ISMs are often used to measure the activities of ions in solutions that are used to calibrate photometric sensors. On the other hand, ISMs cannot track fast changes in ion activity (i.e. in the ms range, but see[13,14]) and in some cases selectivity is a limiting factor. The key component of an ISM is the ion-selective carrier or ionophore, which endows the electrode with the selectivity required to discriminate between ions of similar nature and the sensitivity (usually down to the sub-micromolar range). In contrast to the case for cations, there is a general lack of highly-selective naturally occurring or synthetic anion ionophores, and in particular for Cl^- [15,16].

We tested ISMs made with several commercially available Cl^- ionophores, and unlike our experience with cation ionophores (H^+, Na^+) we found their responses far from ideal. These Cl^- ionophores included: tributyltin (TBT), chloride ionophores I-IV (Selectophore™, Millipore-Sigma), and the antibiotic 3,4,4′-trichlorocarbanilide[17]. We found ISMs fabricated with these compounds had one or more of the following problems: lack of linearity, sub- or supra-Nernstian responses, drift, hysteresis, poor solubility in liquid membranes, sensitivity to blockers of chloride channels or transporters, and poor selectivity for Cl^- over HCO_3^-. We also tested a chemically diverse group of recently published compounds described as Cl^- carriers for biological membranes: compound-1[18], compound 4H[19], cholapod-3, and decalin-13[16,20,21], and found them not appropriate to build ISMs, mostly demonstrating solubility problems.

Here we report that a Cl-selective anion carrier based on a trinuclear Hg(II) complex containing carborane-based ligands, [9]mercuracarborand-3 (MC3), that was previously used in polymer membrane Cl^- sensors[22] is also ideal for liquid membrane Cl-selective ISMs. MC3 is a macrocyclic structure bearing a pre-organized Lewis acid cavity that selectively complexes with Cl^- and functions as an anion carrier in the liquid membrane ISM. We show the MC3-ISM is highly selective for Cl^- over other biologically relevant anions (HCO_3^-, lactate, PO_4^-) and is insensitive to Cl-channel blockers (9-anthracene carboxylic acid), inhibitors of cation-chloride co-transporters (bumetanide, furosemide), or changes in pH and is therefore well-suited for biophysical applications to quantitatively and accurately measure a_{Cl}^i.

Methods

MC3 synthesis. To our knowledge, [9]mercuracarborand-3 (MC3, CAS Registry Number 146219-95-6) is not commercially available and so it was synthesized using air-free Schlenk techniques as described by Hawthorne and co-workers[23]. An oven dried Schlenk flask was charged with 144 mg (0.5 mmol) of *ortho*-carborane (Boron Specialties), filled with an N_2 atmosphere, and 5 mL of anhydrous diethyl ether (Et_2O) (Fisher, inhibitor free) were added via syringe. The reaction vessel was cooled to 0 °C using an ice bath, 0.85 mL of 2.5 M n-BuLi in hexane (Sigma-Aldrich) was added dropwise to the rapidly stirring reaction mixture. After addition of the n-BuLi solution, the ice bath was removed and the reaction was stirred at room temperature for 2 hours. Next, 315 mg of $Hg(OAc)_2$ (Mallinckrodt) was added to the reaction mixture under a flow of N_2 and the reaction mixture was stirred at room temperature for 16 hours. Upon completion of the reaction, the reaction was quenched with 5 mL of H_2O, the organic layer was collected, the aqueous portion was extracted with 5 mL Et_2O. The organic portions were combined and washed with 5 mL H_2O, then the organic layer was dried with $MgSO_4$ and filtered through 2 cm of silica gel using Et_2O as the eluent. The filtrate was evaporated to dryness using a rotary evaporator to yield a white solid. Due to difficulty with purifying the product by recrystallization from Et_2O, an alternative purification method was developed as follows. The white solid was washed with hexanes, dissolved in 10 mL of 20% (v/v) hexanes in Et_2O and left in a fume hood to evaporate the Et_2O portion which resulted in precipitation of an off-white powder. The supernatant was decanted and the solids were loaded onto a 3 cm plug of silica gel wetted with 40% acetone (v/v) in hexanes and eluted with 40% acetone (v/v) in hexanes. The resulting filtrate was evaporated to dryness to yield 50 mg (14% yield) of an off-white solid which contains >95% MC3 by ^{11}B NMR. ^1H NMR (400 MHz, $(CD_3)_2CO$) δ 3.0–1.2 (m). ^{11}B NMR (160 MHz, $(CD_3)_2CO$) δ 1.6 (d, 2B), −5.4 (d, 2B), −8.0 (d, 6B).

Micropipette silanization. Micropipettes were pulled from 1.5 mm borosilicate capillaries with micro-filaments (BF150-86-10, Sutter Instruments). A 4-step pulling protocol was optimized to obtain a short taper (~8 mm) leading to a sub-micron tip opening, using a horizontal puller (P97, Sutter Instruments). When filled with a saline mimicking the ion composition of myoplasm (see solutions), the microelectrodes had tip resistances of 10–12 MΩ. The use of capillaries with micro-filaments greatly reduced the filling-time in the manufacture of ISMs (~5 min compared to >30 min for plain capillaries), without compromising the sealing of the organic phase to the inner surface of the capillary wall. Capillaries were silanized as supplied from the vendor, with no pre-treatment.

For silanization, micropipettes were laid horizontally on a support in a Pyrex glass jar (with lid, ~500 ml). One hundred μl of chlorotrimethylsilane (Sigma) was placed in the jar and allowed to evaporate at RT for ~5 min. The silane vapor had free access to a micropipette's interior and exterior surfaces. Then, the micropipettes were baked at 250 °C for at least 4 h (usually overnight). As occurs with all liquid-junction microelectrodes, silanization was essential to insure the mechanical stability and high electrical resistance between the hydrophobic liquid membrane and the inner wall of an ISM. Silanized micropipettes were stored dry in a closed jar (WPI Jar-E215) to avoid dust adhesion, and were used for up 2 weeks with no noticeable deterioration.

Cl^- sensing liquid membrane and ISM half-cell saline. The ISM liquid membrane consisted of a short column (200–300 μm) of a hydrophobic "chloride cocktail" lodged in the tip of the micropipette. The chloride cocktail was made by dissolving the MC3 and a lipophilic cationic additive (tridodecylmethyl ammonium chloride, TDMAC, Sigma) in the water - immiscible organic solvent 2-nitrophenyl octyl ether (NPOE, Sigma). We

used 10% MC3 and 2.5% TDMAC in NPOE (w/volume). No other mixing ratios or solvents were studied. The ISM half-cell consisted of 100 mM NaCl, backfilled into the microelectrode and in contact with an Ag/AgCl reversible electrode.

ISM fabrication. We devised a simple and efficient method to fabricate ISMs. Starting with previously silanized micropipettes, we routinely made six ISMs in less than 1 h. To fabricate an MC3-ISM both the chloride cocktail and the reference saline were sequentially backfilled into the micropipette, while viewing under a stereomicroscope. First, an excess amount of chloride cocktail (2–3 times the final volume of the liquid membrane) was delivered as close as possible to the micropipette tip using a 34G microneedle (Quickfil 34G-5, WPI, for which the polyimide coating was stripped from the end). The organic phase spontaneously moves towards the tip of the micropipette by capillary action and fills the shaft in 3–5 min. Initially using excess chloride cocktail speeds up this filling step. Once the tip is filled, the chloride cocktail volume is reduced as much as possible by suction with a new 34G needle. Finally, the saline solution is delivered (using another 34G needle), assuring that a clean interface is formed between the two liquids. Care must be taken to avoid air bubbles in the organic phase or interface, otherwise the ISM should be discarded.

Prior to use, each MC3-ISM was individually tested using a 3 point calibration including solutions of 1, 10 and 100 mM Cl (see solutions), with a_{Cl} of 0.64, 6.46, and 68.5 mM respectively. Tested MC3-ISMs were stored in closed jars (to avoid evaporation and dust) with tips submersed in a filtered (0.2 μm) solution containing 10 mM NaCl; and could be used after 1–2 weeks from fabrication with no detectable deterioration.

Measurement of ISM potential. A two-channel high input impedance ($>10^{15}\,\Omega$) amplifier (FD223a, WPI) was used to measure the electrical potential of MC3-ISMs. One channel was connected to the Ag/AgCl wire of an MC3-ISM. The second channel was connected to a standard ("sharp") microelectrode having 10–15 MΩ tip resistance when filled with electrode solution (see solutions). This microelectrode served as a reference electrode, whose value (V_{ref}) reflects changes in junction potential that may occur upon solution exchanges. Three amplifier outputs, V_{ref}, V_{ISM}, and the analog difference $V_{ISM} - V_{ref}$ were digitized with a 16-bit A/D converter and stored on a computer (LabVIEW, National Instruments). The figures show V_{Cl}, defined as $-(V_{ISM} - V_{ref})$, because with this sign convention the potentiometric signal increases for an increase in a_{Cl}.

Solutions. Solutions containing different [Cl⁻] were prepared in two ways: (1) Calibration solutions devoid of any possible interfering anion were prepared by serially diluting a pure NaCl solution with distilled water (18 MΩ-cm, Millipore). (2) Calibration solutions suitable for use with mammalian cells were prepared by mixing two solutions having a composition similar to that of Tyrode's buffer but differing in the main anion content, and having the same pH and divalent cation content. These solutions differ in that one (150 - Cl solution) contained Cl⁻ as the main anion, and the other (0 - Cl solution) was devoid of Cl⁻, and contained SO_4^{-2} as the main anion. Both solutions have HEPES (a possible interfering anion) as the pH buffer.

$$\text{150-}Cl\ solution\ (mM)\text{: }140\ NaCl,\ 4\ KCl,\ 2\ CaCl_2,\ 1\ MgCl_2,\ 10\ HEPES;$$
$$\text{pH} = 7.4\ \text{with NaOH.}$$

$$\text{0-}Cl\ solution\ (mM)\text{: }115\ Na_2SO_4,\ 2\ K_2SO_4,\ 2\ Ca(OH)_2,\ 1\ Mg(OH)_2,\ 10\ HEPES;$$
$$\text{pH} = 7.4\ \text{with }H_2SO_4.$$

Calibration solutions containing from 100 mM to 10 nM nominal Cl concentrations were made by serial dilutions of the 150 − Cl solution with the 0 − Cl solution.

Solutions containing potential interfering anions were prepared by adding 10 mM of Na-lactate, NaHCO₃, Na₂HPO₄ or NaSCN to a mixture of the 150 − Cl and 0 − Cl solutions, and then performing a similar serial dilution as described above to obtain the desired [Cl⁻]. Drug-containing solutions were made from highly concentrated stock solutions of 9-anthracenecarboxylic acid (9-ACA, 500 mM in DMSO) or bumetanide (BMT, 50 mM in DMSO). DMSO final concentration was kept below 1:1000, and controls were run to exclude direct effects of solvent.

Solutions used for recording from isolated mouse muscle fibers were either standard (i.e. Cl-containing) Tyrode's solution or Cl-free Tyrode's in which the Cl⁻ was replaced with SO_4^-. Standard Tyrode's (mM): 150 NaCl, 4 KCl, 2 CaCl₂, 1 MgCl₂, 10 glucose, 10 HEPES; pH = 7.4 with NaOH. Cl-free Tyrode's (mM): 115 Na₂SO₄, 2 K₂SO₄, 2 Ca(OH)₂, 1 Mg(OH)₂, 10 HEPES; pH = 7.4 with H₂SO₄. A salt bridge was used to connect the bath of the recording chamber to the reference ground, so that shifts in the junction potential were minimized when bath exchanges were used.

The MC3-ISM was backfilled with a solution containing (in mM): 100 NaCl, 10 HEPES, pH = 7.4 with H₂SO₄. The reference (bath) and intracellular microelectrodes were filled with a solution (in mM): 60 K-aspartate, 5 di-Na ATP, 5 di-tris creatine phosphate, 40 EGTA, 20 MOPS, 5 MgCl₂, pH = 7.4 with KOH.

All chemicals were purchased and used as received from Millipore-Sigma, unless otherwise noted (*vide supra*).

Cl⁻ activity calculation (a_{Cl}). The value for the activity of an ion in solution, a_{ion} is often obtained from tables[24], but these values were calculated from solutions of single salts (e.g. NaCl, KCl). Instead, we calculated a_{Cl} (in mM) for all simple and mixed solutions as: $a_{Cl} = \gamma_{Cl} * [Cl]$, where γ_{Cl} is the chloride activity coefficient (dimensionless). The activity coefficient was calculated from the extended Debey-Hückel[25] formalism as:
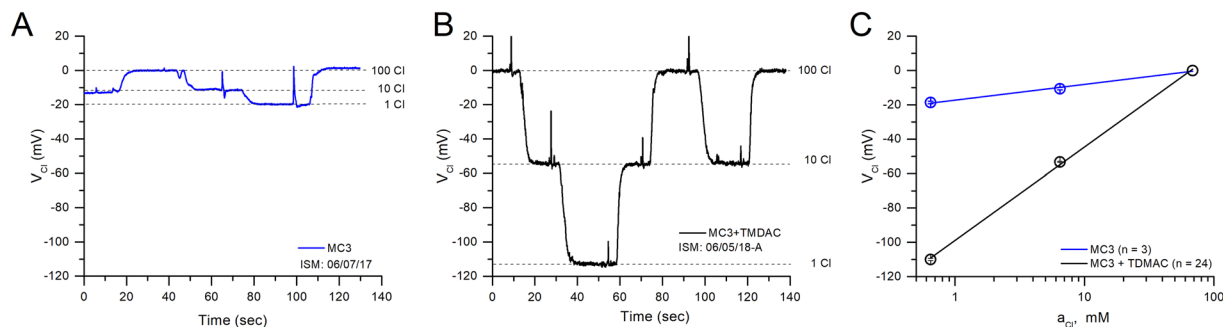
Figure 1. TDMAC is required for Nernstian behavior of the MC3-ISM. (**A**) Response of an exemplary ISM for which the liquid membrane consisted only of 10% MC3 dissolved in NPOE, as the [Cl⁻] was varied from 1 to 100 mM. (**B**) Response of another ISM containing the same liquid membrane as in A, but supplemented with 2.5% TDMAC. The rapid transients for the tracings in (**A,B**) were caused by solution switching and suction-dependent fluctuations. (**C**) Plot of V_{Cl} as a function of $\log_{10}(a_{Cl})$ shows a linear relation with a slope of 54.6 ± 0.18 mV (n = 24) for the ISMs containing TDMAC (black circles), as expected for a Nernstian response. For ISMs lacking TDMAC (blue circles), a sub-Nernstian response was observed with a slope of 9.2 ± 0.67 mV (n = 3). The error bars for the SEM are very small, and obscured by the symbols.

$$\log(\gamma_{Cl}) = \frac{-A z_i^2 \sqrt{Is}}{1 + B \delta_{Cl} \sqrt{Is}}$$

where δ_{Cl} is the effective Cl⁻ ion diameter (0.3 nm), $A = -0.510$, and $B = 3.29$. The ionic strength, Is, of a solution containing many ions, ion_i, with valences z_i was calculated as:

$$Is = \frac{1}{2} \sum_i [ion_i] z_i^2$$

"In cuvette" MC3-ISM characterization.   A small circular plastic experimental chamber (8 mm in diameter, 1 mm depth, ~0.5 ml in volume) was used to study the response of MC3-ISMs to [Cl⁻] changes and to determine selectivity. The chamber was continuously perfused with the test solution of choice and the entire chamber could be completely exchanged in ~1 sec. Perfusion flux (standard of 1–2 ml/min) was driven by gravity and the efflux was removed by aspiration, keeping the level of solution constant to minimize drifts in junction potentials. The chamber solution was connected to ground via a salt bridge (3% agar in 125 mM KCl, w/v containing a floating platinum wire) in contact with a 125 mM KCl solution and an Ag/AgCl electrode. This arrangement represented the second (electrical) half-cell across the MC3-ISM's liquid membrane.

Muscle fiber ISM measurements.   To test the MC3-ISM in a cellular context, we used enzymatically dissociated skeletal muscle fibers from the flexor digitorum brevis (FDB) of the mouse, as previously described[26]. All mouse procedures were approved by the University of California Los Angeles Institutional Animal Care and Use Committee. All methods performed in this study were conducted in accordance with the guidelines and regulations of the IACUC. Fibers were plated in the same chamber as above, and impaled with a MC3-ISM and a reference micro-electrode. Before impalement, both MC3-ISM and reference micro-electrode were zeroed in the presence of 100 − Cl Tyrode.

Selectivity coefficient, $K_{Cl,X}^{pot}$.   The relative selectivity of an MC3-ISM for Cl⁻ over a test interfering anion was determined by the fixed interference method[27]. The concentration of the test interfering anion, [X⁻], was maintained at a fixed value of 10 mM, and the MC3-ISM /potential was measured as the [Cl⁻] was varied from 10 nM to 100 mM. The MC3-ISM potential was plotted against $\log(a_{Cl})$ and the intersection of the two linear portions (Nernstian for high [Cl⁻] and saturating for low [Cl⁻]) determined the value of a_{Cl} that was used to calculate the selectivity coefficient for Cl⁻ over X⁻ as:

$$K_{Cl,X}^{pot} = a_{Cl} / a_X^{z_{Cl}/z_X}.$$

Values are reported as the mean ± standard error of the mean.

Results

A cationic additive increases the Cl⁻ responsiveness an MC3-based ISM.
We first tested the response of liquid membrane ISMs constructed using a cocktail containing only MC3 (10%) and NPOE. These electrodes were only weakly sensitive to [Cl⁻] changes, as shown for an exemplary response in Fig. 1A. This response is sub-Nernstian, with a slope of 9.2 ± 0.67 mV/decade (n = 3) on a plot of V_{Cl} as a function of $\log_{10}(a_{Cl})$ (Fig. 1C, blue symbols). This result is in agreement with previous data[22], demonstrating that polymeric membranes containing MC3 are insensitive to Cl⁻ unless the membranes are doped with cationic compounds.
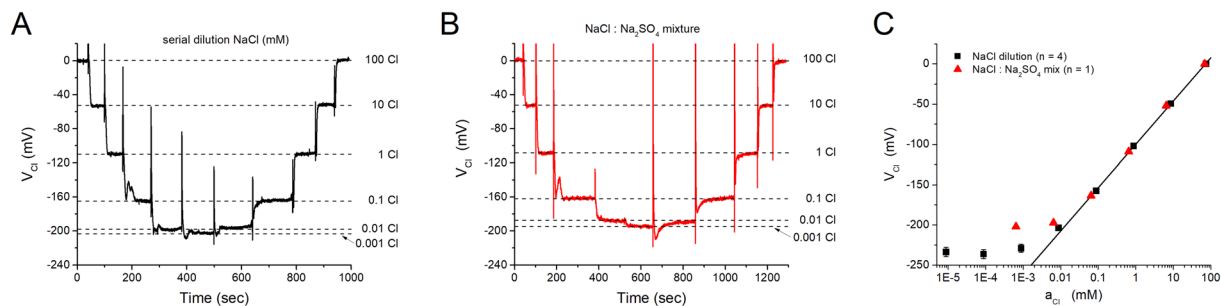
Figure 2. MC3-ISMs have a linear response to [Cl⁻] changes from 0.1 to 100 mM. (**A**) Continuous record of the response (V_{Cl}) for an MC3-ISM exposed to solutions of various [Cl⁻] from 0.001 mM to 100 mM, obtained by serial dilutions of a 100 mM NaCl solution with water. (**B**) Continuous record of another MC3-ISM exposed to the same nominal [Cl⁻], but obtained by mixing Cl-based and SO₄-based solutions (see Methods). The dashed lines in (**A,B**) represent the steady state values of the ISMs at the indicated [Cl⁻]. (**C**) The steady-state V_{Cl} is plotted as a function of a_{Cl}, which was calculated on the basis of the ionic strength of the test solutions (See Methods). A linear fit of V_{Cl} as a function of a_{Cl} over a range from 0.088 to 75 mM, for the dilution method, had a slope of 52.8 ± 0.63 mV/decade (n = 4, straight line).

When the liquid membrane cocktail was supplemented with a lipophilic cationic additive, TDMAC (2.5%, w/w), the potentiometric response became highly sensitive to [Cl⁻] changes between 1 and 100 mM (Fig. 1B). For brevity, we refer to microelectrodes with this complete liquid membrane cocktail as MC3-ISMs, but it should be recognized they are doped with TDMAC. The voltage response of MC3-ISMs was stable and showed no signs of hysteresis. Over this range of [Cl⁻], the MC3-ISM response was nearly Nernstian, with a slope of 54.6 ± 0.18 mV/decade (n = 24), as shown in Fig. 1C (black symbols). The reference electrode had very small voltage changes in response to these solution exchanges (2–3 mV, not shown), and these small deviations were subtracted from V_{ISM} to obtain V_{Cl} values shown in Fig. 1.

We did not explore other combinations of MC3 and TDMAC since the 10% and 2.5% (w/w), respectively, mixture tested gave optimal results. The need for a lipophilic cation stems from the fact that MC3 is a neutral carrier, and as such it is expected to produce a limited anion response unless a counterion for the mercuracarborand complex is added[22].

Linearity and Cl⁻ detection limit of the MC3-ISM.
The linear range for Cl⁻ responsiveness of the MC3-ISM was determined by changing the [Cl⁻] over 7 orders of magnitude, in ten-fold steps from 100 mM to 10 nM. This calibration was performed with solutions prepared by serial dilution of 100 mM NaCl with water (Methods) to minimize the possibility of interfering anions at low concentrations of Cl⁻. A typical continuous recording of V_{Cl} during the decrease and then increase of [Cl⁻] is shown in Fig. 2A. Jumps of V_{Cl} to new stable values are clearly evident with each solution exchange, and the dotted lines emphasize that no hysteresis was detected. The change in V_{Cl} became compressed (i.e. smaller jumps) for test solutions of less than 0.1 mM [Cl⁻], as the linear range was exceeded.

A limited number of trials were also performed with solutions prepared by serially diluting 100 mM NaCl with a Na₂SO₄-based solution (Fig. 2B) that is commonly used for "chloride-free" conditions in studies on skeletal muscle fibers (Methods, 0 – Cl solution). This alternative method maintains a high ionic strength for all test values of [Cl⁻] and provides a check for evidence of interfering anions in a mammalian physiologic buffer. A plot of steady-state V_{Cl} as a function of $\log_{10}(a_{Cl})$ shows that between 0.1 mM and 100 mM the response was linear (Fig. 2C). This range exceeds the expected values of intracellular a_{Cl} to be encountered in mammalian cells (3 to 20 mM, or even up to 100 mM in pathological contexts such as glioma[28]). Moreover, the response for dilutions with pure water was near-linear down to an activity of 0.01 mM. The saturation of V_{Cl} at about −200 mV for the NaCl: Na₂SO₄ mixture reveals an interfering anion effect of SO_4^{-2}, although this was detectable only at low a_{Cl} levels (<0.1 mM) that are not encountered in cells.

The average slope of the linear response range was 52.8 ± 0.63 mV/decade (n = 14). While this slope is slightly smaller than the theoretical value of 58 mV, it is comparable to values reported for MC3 electrodes fabricated in solid membranes[22]. Those electrodes also showed a sub-Nernstian response, with the slope being smaller for lower molar ratios of TDMAC to MC3.

The settling time for an MC3-ISM is a few seconds.
Another desirable feature of ISMs for biological applications is a small time constant. To assess the time response of the MC3-ISM, we increased the flow rate of the solutions perfusing the experimental chamber (40 ml/min), as compared with those used in experiments in Figs. 1 and 2. The continuous flow was briefly switched from a 100 mM Cl⁻ solution to a 10 mM Cl⁻ solution that also contained fluorescein (100 μM). Local spot illumination (100 μm diameter disc, λ = 488 nm) near the tip of the MC3-ISM was used to simultaneously measure the kinetics of the bath exchange while the MC3-ISM response was recorded. On average, the fluorescence transient decayed with a time constant of 1.1 ± 0.15 sec (n = 4) and after a brief lag, V_{Cl} decayed almost as quickly, 1.4 ± 0.26 sec (n = 4), as shown by the exemplary responses in Fig. 3. Thus even at this high flow rate, the response time of our MC3-ISM is limited by solution exchange, and we can conclude that the intrinsic time constant of the ISM is smaller than 1.4 sec.
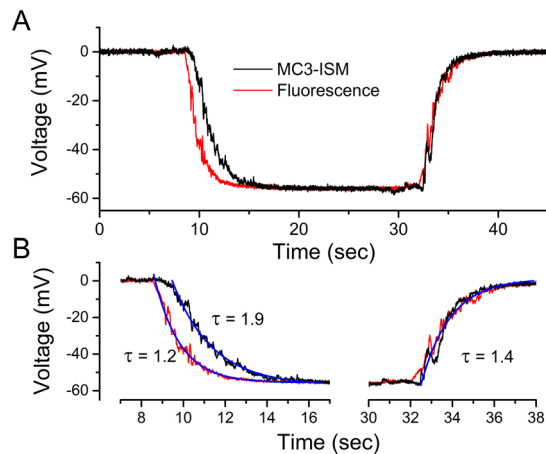
Figure 3. Liquid-membrane MC3-ISMs respond rapidly to [Cl⁻] changes. (**A**) Simultaneous recording of V_{Cl} and the solution exchange, when the continuous flow of 100 mM Cl⁻ was briefly switched to 10 mM Cl⁻ (9 to 33 sec interval) and back. Flow was detected by adding fluorescein (100 μM) to the 10 mM Cl⁻ solution and exciting with local spot illumination (100 μm disc) near the ISM tip. Signals were sampled at 50 Hz, and the amplitude of the fluorescence signal was scaled to provide a direct comparison of kinetics by superimposing the traces. (**B**) Onset and offset of the 10 mM Cl⁻ exchange are shown on an expanded time scale, along with exponential fits.

The response time of a liquid-junction ISM is usually faster as the width of the organic phase decreases at the tip of the electrode[13,14]. The width for the liquid membrane of our MC3-ISMs was ~300 μm, and we did not explore whether the time constant could be reduced by decreasing the width of the organic phase. In any event, a time response in the order of a few seconds is sufficient to study intracellular [Cl⁻] changes expected to occur in several tens of second to minutes in biological settings.

The MC3-ISM is insensitive to changes in pH or HCO_3^-.   One of the biggest drawbacks of available Cl⁻ sensing ISMs is their sensitivity to HCO_3^- [29]. The problem posed by HCO_3^- is complex. This ubiquitous intracellular anion is more abundant than Cl⁻ in many cells (e.g. 3-fold higher in mammalian skeletal muscle), and the [HCO_3^-] varies greatly depending on pH and pCO_2 changes. Consequently, for Cl-sensing ISMs that are also sensitive to HCO_3^- there is no simple way to distinguish between real a_{Cl} changes, and spurious potential shifts caused by changes in [HCO_3^-]. Early Cl-sensing ISMs based on anion exchangers had notoriously poor selectivity for Cl⁻ over HCO_3^- [15]. Selectivity for Cl⁻ was greatly improved by using anion-selective carriers, e.g. Mn(III) porphyrins[30], but the physiochemical properties of these first-generation carrier electrodes were unfavorable with instability, drift, and non-Nernstian behavior. The high selectivity for Cl⁻ over HCO_3^- and near-Nernstian behavior of MC3-based solid membrane electrodes[22] showed tremendous promise for developing a Cl-selective liquid membrane ISM suitable for biological applications.

We measured the sensitivity of MC3-ISMs to interference from changes in pH or [HCO_3^-], as a test of suitability for these ISMs to be used for intracellular determination of a_{Cl}. First, we tested for MC3-ISM sensitivity to ΔpH from 6.5 to 8.5, which covers the entire physiologic range of expected cytoplasmic values. In these HEPES-buffered HCO_3^- - free solutions, a three-point Cl⁻ calibration response (1, 10, 100 mM) for an MC3-ISM was not affected by a pH shift from 7.4 to 6.5 or from 7.4 to 8.5 (Fig. 4A, *left* and *right*, respectively). Next, we measured the response of MC3-ISMs in constant 10 mM Cl⁻, a typical value for myoplasmic Cl⁻ in skeletal muscle fibers[31,32], upon which was imposed step changes in HCO_3^- from 1 to 50 mM (Fig. 4B), a concentration range far beyond those expected to occur *in vivo* either in physiological or pathological conditions (i.e. ~13 mM[33]). The potentiometric response of MC3-ISMs was completely insensitive to the presence of HCO_3^- at concentrations as high as 50 mM. This is a remarkable feature of the MC3 Cl-selective carrier, and makes MC3-based ISMs the electrode of choice for biological purposes.

Chloride selectivity of the MC3-ISM.   The selectivity of the MC3-ISM was assessed for Cl⁻ over various physiologically relevant anions including lactate, phosphate, thiocyanate and bicarbonate. The fixed interference method, as described by IUPAC was used[27], wherein the concentration of the test interfering anion was held constant at 10 mM (as a Na⁺ salt), and V_{Cl} was measured in solutions with varying [Cl⁻] between 100 mM and 100 nM. We found that the MC3-ISM response is not significantly affected by the presence of lactate, phosphate, or bicarbonate for [Cl⁻] from 100 mM to values as low as 100 μM (Fig. 5). On the other hand, the MC3-ISM was almost insensitive to Cl⁻ in the presence thiocyanate (Fig. 5, magenta diamonds). From the data in Fig. 5, we calculated the selectivity coefficient, $K_{Cl,X}^{pot}$, for each test anion (Table 1) which gives a selectivity series: thiocyanate > Cl ≫ bicarbonate > phosphate ≈ lactate. Importantly, the MC3-ISM was 125-fold more sensitive to Cl⁻ than to HCO_3^-, which explains the lack of an effect for HCO_3^- in Fig. 4 and confirms the MC3-ISM is suitable for measuring intracellular a_{Cl} without interference from fluctuating levels of HCO_3^-.
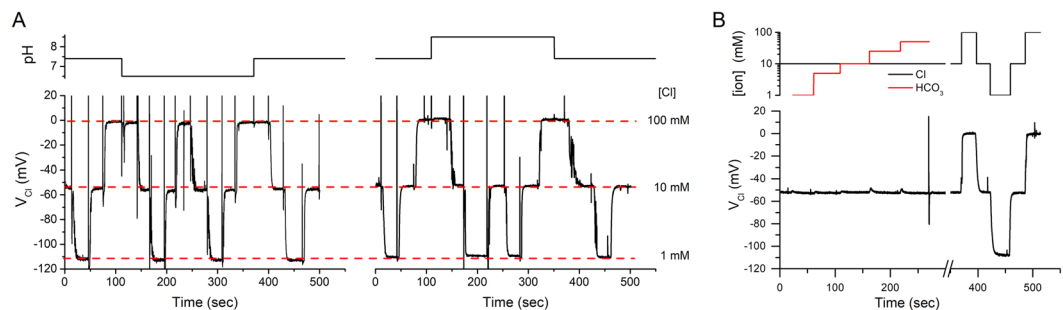
Figure 4. The MC3-ISMs are insensitive to changes in pH or HCO_3^-. (**A**) The Cl^- responsiveness of an MC3-ISM was not affected by pH changes from 6.5 to 8.5 units. The left panel shows the three-point calibration response of V_{Cl} for $[Cl^-]$ of 1, 10, and 100 mM is identical at pH 7.4 or pH 6.5 (depicted in the upper plot). Similarly, the right panel shows that the Cl^- calibration response was not affected by a pH change from 7.4 to 8.5 units. (**B**) The left portion of the V_{Cl} trace (0 to 300 s) shows the MC3-ISM response in 10 mM Cl^- remained constant, as the $[HCO_3^-]$ was varied in step increments from 1 mM to 50 mM. The pH for these NaCl: NaHCO$_3$ mixtures varied from 7.2 to 7.68, indicating the pCO$_2$ of the solution had not fully equilibrated with room air. The right part of the record ($>$350 sec) is the response of this same electrode to changes in $[Cl^-]$ in the absence of HCO_3^-. The changes in HCO_3^- and Cl^- are depicted in the upper panel by the red and black traces, respectively. For all panels, the different $[Cl^-]$ were obtained by mixing Cl-based and SO$_4$-based solutions (Methods). The "spikes" in the records are due to flux-dependent artifacts during solution switching.
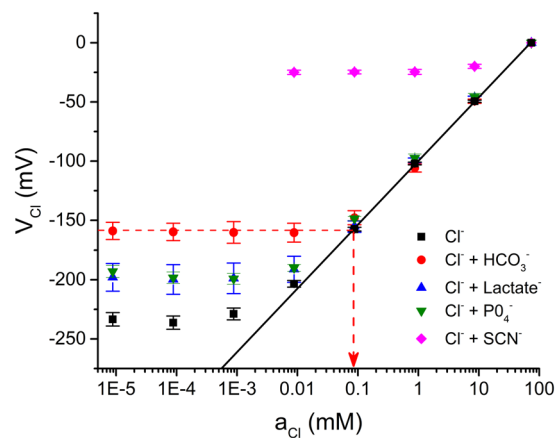

Figure 5. The MC3-ISM is highly selective for Cl^-. The MC3-ISM response was measured in solutions prepared by serial dilution of pure NaCl with no interfering anions (n = 14, black squares reproduced from Fig. 2) or for the NaCl solutions plus 10 mM of the test anion as Na$^+$ salts of HCO_3^- (n = 3, red circles), lactate (n = 3, blue triangle), PO_4^- (n = 3, green inverted triangle), or SCN^- (n = 3, magenta diamond). A linear fit for the pure NaCl data over a range of 0.1 mM to 100 mM solutions shows a Nernstian response (black line). The cut-off a_{Cl} in the presence of an interfering anion was determined by the intersection of limiting asymptote and the Nernstian response, as shown by the example for HCO_3^- (red dashed line). These values were used to calculate the selectivity coefficient (see Methods).

Anion	a_{Cl}, (mM)	$K_{Cl,anion}^{pot}$	$log_{10}(K_{Cl,anion}^{pot})$
SCN$^-$	26 ± 2.1	2.8 ± 0.23	0.45 ± 0.035
HCO$_3^-$	0.091 ± 0.010	0.010 ± 0.0012	−2.0 ± 0.052
Lactate	0.014 ± 0.0077	0.0015 ± 0.00085	−3.0 ± 0.24
PO$_4^-$	0.010 ± 0.0028	0.0011 ± 0.00031	−3.0 ± 0.15

Table 1. Anion selectivity coefficients of the MC3-ISM.

Chloride channel blockers and inhibitors of Cl^- co-transporters have little effect on the MC3-ISM response.

Chloride-selective electrodes are often sensitive to blockers of Cl^- channels or to inhibitors of Cl^- co-transporters[31,34,35]. We assessed the MC3-ISM sensitivity for three commonly used Cl^- agents, the ClC-1 blocker 9-ACA and the NKCC1 inhibitors bumetanide (BMT) or furosemide (FUR). Our test for
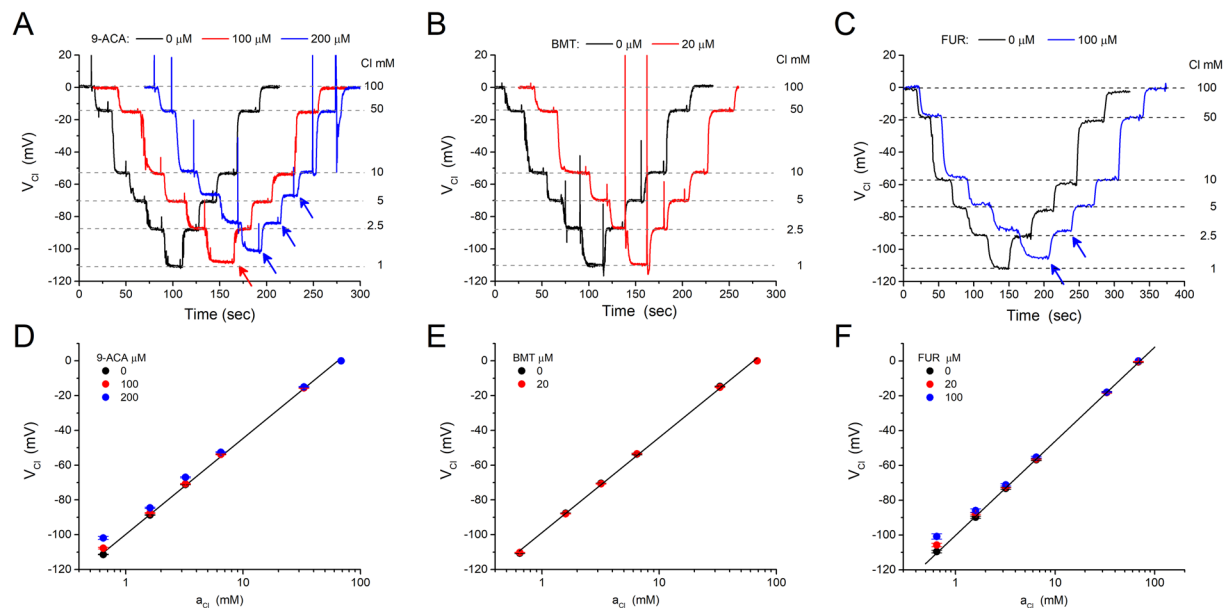
Figure 6. The MC3-ISM response is minimally affected by a Cl⁻ channel blocker and Cl⁻ cotransporter inhibitors. (**A**) Continuous records of the MCS-ISM potential (V_{Cl}) in response to step changes of [Cl⁻] (1, 2.5, 5, 10, 50, 100 mM) in the absence (black trace) or presence of 100 μM (red trace) and 200 μM (blue trace) 9-ACA. Records for each 9-ACA concentration were obtained consecutively for the same MC3-ISM, but were shifted in time and superimposed to facilitate a visual comparison. Arrows indicate detectable differences from the control response in the absence of 9-ACA. (**B**) Addition of 20 μM bumetanide (BMT) did not detectably alter the V_{Cl} response of an MC3-ISM. The test protocol and display of the continuous data were the same as in (**A**). (**C**) Addition of 100 μM furosemide (FUR) did not affect the response for Cl⁻ solutions of 5 mM or greater, and mildly attenuated the response in 2.5 and 1 mM solutions (blue arrows). (**D–F**) Calibration plots of V_{Cl} as a function of a_{Cl} shows that a modest shift of V_{Cl} was detectable only for 200 μM 9-ACA and at the lowest concentration test solution with 0.1 mM Cl⁻. For each drug tested (**A–C**), similar responses were observed for four different MC3-ISMs. Symbols represent the mean ± SEM for 4 different MC3-ISMs.

interference was based on detecting a distortion of the Nernstian behavior of an MC3-ISM over an operating range of 1 mM to 100 mM [Cl⁻], while the Cl⁻ agents were added at concentrations typically used for studies of muscle. We found that the MC3-ISM is almost insensitive to 9-ACA (Fig. 6A,D), with a very small effect (reduced V_{Cl} response) in 200 μM 9-ACA when [Cl⁻] was 5 mM or lower. Studies in skeletal muscle that are designed to eliminate the ClC-1 conductance typically use 100 μM 9-ACA[36]. With this concentration of blocker, the V_{Cl} response remained Nernstian down to a [Cl⁻] of 2.5 mM (the lowest expected physiologically), demonstrating that MC3-ISMs can be used to measure intracellular a_{Cl} in studies with 9-ACA. The MC3-ISM response was insensitive to BMT (Fig. 6B,E). At 20 μM, a concentration in 10-fold excess of that used for complete inhibition of NKCC1, there was no detectable distortion of the MC3-ISM Nernstian behavior over a [Cl⁻] range from 1 mM to 100 mM. BMT concentrations up to 100 μM have been used for some investigations[37], although in our experience this approaches the solubility limit in physiological saline. Even for a 1:500 dilution of a 50 mM stock BMT solution in DMSO (nominally 100 μM BMT), the MC3-ISM was distortion-free down a [Cl⁻] of 2.5 mM. The MC3-ISM response was mildly attenuated in the presence of 100 μM FUR in Cl⁻ solutions of 2.5 mM and lower (Fig. 6C,F).

Intracellular Cl⁻ activity, a_{Cl}^i, measured with an MC3-ISM.

We verified the performance of the MCS-ISM as a sensor of intracellular Cl⁻, by recording a_{Cl}^i in a skeletal muscle fiber isolated from the flexor digitorum brevis of the mouse. The fiber was impaled with a standard reference electrode to measure the resting potential (V_m Fig. 7, upper panel) and also with a Cl-selective MC3-ISM (V_{ISM}) which reports the combined effect of V_m and V_{Cl}. The offset for $V_{ISM} = 0$ mV was set in a calibration solution with 100 mM [Cl⁻]. The difference between these two signals, $V_{Cl} = V_m - V_{ISM}$ (Fig. 7, lower panel) is proportional to $log_{10}(a_{Cl}^i)$.

In control Tyrode solution (140 mM Cl⁻), the resting membrane potential was stable ($V_m = -80$ mV), as was $V_{Cl} = -65$ mV, corresponding to $a_{Cl}^i = 6$ mM. Upon switching the perfusion to SO₄-Tyrode (nominally zero Cl⁻) the intracellular a_{Cl}^i exponentially fell to about 1.5 mM because of Cl⁻ efflux through the high resting conductance of ClC-1 channels. These changes are fully reversible, as shown by the recovery of a_{Cl}^i when the perfusion with Cl⁻ Tyrode was resumed at 500 sec in Fig. 7.

The transient response of V_m is also consistent with decrease of a_{Cl}^i, followed by recovery[4]. At the onset of Cl-free Tyrode solution (Fig. 7, 80 sec), V_m depolarized because the equilibrium potential for Cl⁻ suddenly shifted from about −77 mV to a positive value. Intracellular Cl⁻ content then declined over the next 30 s, which shifted E_{Cl} to more negative potentials and caused V_m to relax back toward −80 mV. When extracellular Cl⁻ is suddenly
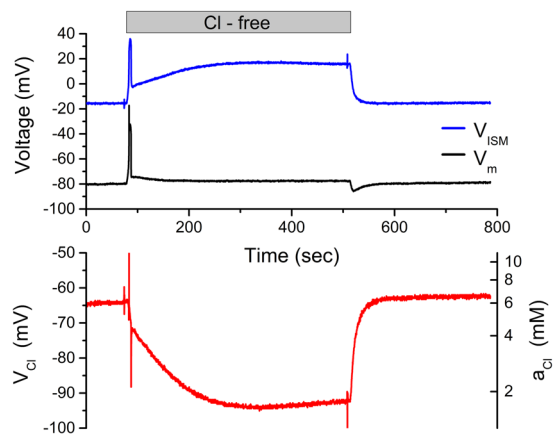
Figure 7. Myoplasmic a_{Cl}^i measured with an MC3-ISM. Simultaneous intracellular recordings of membrane potential (V_m, black trace) and the MC3-ISM response (V_{ISM}, blue trace) were obtained by impaling a dissociated fiber from the flexor digitorum brevis muscle (upper panel). Digital subtraction ($V_m - V_{ISM}$) was performed to calculate the red trace in the lower panel, representing both linear changes of V_{Cl} (left ordinate) as a function of time and logarithmic changes in a_{Cl}^i as a function of time (right ordinate). At 80 s, the bath was exchanged to Cl-free Tyrode solution, and then back to normal Tyrode (150 mM Cl) at 500 s.

restored (Fig. 7, 500 sec), V_m had a hyperpolarizing undershoot because intracellular a_{Cl}^i was now lower than baseline. As a_{Cl}^i increased back to the normal basal level, V_m relaxes to the initial value of -80 mV. Similar responses were observed in 8 additional muscle fibers.

Discussion

The development of a highly-selective and sensitive chloride sensor in polymeric membrane electrodes, based on the preorganized macrocyclic Lewis acid MC-3 as the anion carrier[22], was a major technological advance. Prior electrode designs using anion exchangers (e.g. TBT or TDMAC) lacked selectivity, which in these electrodes was dominated by anion lipophilicity (Hofmeister series). Improved Cl⁻ selectivity was achieved with metalloporphyrin carriers (e.g. Mn(III), chloride ionophore I Sigma-Aldrich), but interference from HCO_3^- was still problematic, $log_{10}(K_{Cl,HCO3}^{pot}) = -1.4$, for intracellular determination of a_{Cl}[38]. Excellent selectivity for Cl⁻ over HCO_3^- was achieved with neutral carriers comprised of Lewis acids containing two or more covalently bonded Hg(II)[39] (e.g. chloride ionophore II, Sigma-Aldrich), but these compounds were suboptimal for liquid membrane ion-selective microelectrodes because of sluggish response times ($t_{90\%} \sim 10\,s$), electrical instability with drift and non-Nernstian responses, or poor solubility in NPOE. In contrast, MC-3 is chemically stable, and MC-3 based polymeric membrane electrodes have more consistent Nernstian responses, high selectivity for Cl⁻, and faster settling times of a few seconds. The MC3 ionophore represents a unique platform for chloride sensing. These properties stem from the molecular architecture of this structure which includes a precise triatomic arrangement of Hg(II) sites separated by rigid *ortho*-carboranyl boron-rich cluster ligands. Such a trinuclear metal receptor arrangement allows MC3 to bind anions in a multivalent fashion. Furthermore, electron-withdrawing nature of the C-bound *ortho*-carborane clusters, similar in magnitude to the perfluoroaryl substitutents[40,41], enhances the Lewis acidity of the Hg(II) centers critical to the anion binding. Finally, the sterically encumbering nature of the boron cluster ligands enhances the kinetic stability of the corresponding organometallic complex and creates a well-defined pocket around the Hg-based centers modulating the anion binding selectivity.

We now show that the advantages of MC-3 based polymeric membrane electrodes can be realized in a liquid membrane microelectrode form factor. Following from the design of the MC-3 electrodes in PVC membranes[22], we used NPOE as the liquid organic phase in our ISMs and no other plasticizers were tested. Just as with the PVC membrane electrodes, the potentiometric response to Cl⁻ with MC-3 alone was sub-Nernstian (Fig. 1), and doping the liquid membrane with a lipophilic cationic additive (2.5% TDMAC) markedly increased the ISM sensitivity to near-Nernstian behavior (54.3 mV/decade). Increased amounts of cationic additive in PVC membrane electrodes extended the linear range for high a_{Cl} to about 100 mM, but with a cost of slightly reduced selectivity for Cl⁻ over other anions[22]. Since our ISMs already had linear responses up to the highest concentration of the calibration solution (nominally 100 mM mixture, calculated $a_{Cl} = 68.5$ mM), we did not test higher amounts of additive. Moreover, in a physiological context the expected intracellular a_{Cl} is in the range of 3 to 20 mM.

The potentiometric responses of MC-3 ISMs were remarkably consistent and stable over long recording periods. Except for the occasional failure in the fabrication of an ISM (e.g. air bubble at the liquid membrane/aqueous electrolyte interface), the variability was exceptionally small in the slope of the linear response range (0.1 mM to 100 mM). A sample of 24 MC-3 ISMs with an average slope of 54.6 mV/decade had a standard deviation of only 0.9 mV/decade and a range of 52.9 to 56.0 mV/decade. By comparison, a sample of 62 ISMs constructed with the "improved" Corning 477913 chloride ionophore was reported to have a mean slope of 52.8 mV/decade with a standard deviation of 5.1 mV/decade and the range of values extended from 35 to 64 mV/decade[42]. The potentiometric response of MC-3 ISMs was stable with no significant drift over ten minutes or more, as shown

by examples in several Figs. (2–4, 6). Moreover, the intracellular response recorded from a skeletal muscle fiber was also stable, as shown by the return to the baseline value after recovery from a 10 min exposure to Cl-free conditions (Fig. 7).

The slow electrical response time of Cl-selective ISMs has been a limiting factor for use of some ionophores. The problem arises from the high resistivity of immiscible liquid membranes with neutral ion carriers in combination with the capacitance of the glass pipette. While reducing the ISM tip resistance with cationic additives, choice of the ionophore, and optimization of the liquid membrane thickness may be used to improve performance, the 10% to 90% response time was reported to be as long as 41 sec for Mn(III) porphyrin Cl-selective ISMs[38]. For macroscopic MC-3 electrodes in PVC membranes, a more favorable rise time of about 10 sec was observed[22]. In our MC-3 ISMs the 10% to 90% response time was about 3 sec (Fig. 3), which is sufficient to monitor changes of intracellular a_{Cl} in muscle fibers that typically occur over tens of seconds to minutes.

The most important advantage of MC-3 ISMs is the high selectivity for Cl over other anions, especially HCO_3^-. Historically, the Cl$^-$ ISMs used in several landmark papers showing intracellular a_{Cl} in muscle and heart is higher than expected from passive electrodiffusion were based on proprietary Cl$^-$ ionophores from Corning (477315 and later 477913) that had substantial interference from HCO_3^- [29,31,32]. This limitation was compounded by the composition of the intracellular milieu, where a_{Cl} is typically 4 mM, and HCO_3^- is more abundant at 14 to 18 mM. With a Corning 477913 ISM, the selectivity for Cl over HCO_3^- was about 8:1, corresponding to a selectivity coefficient $\log_{10}(K^{pot}_{Cl,HCO3})$ of -0.9[38]. With this degree of HCO_3^- interference, a true a_{Cl} of 4 mM in combination with an a_{HCO3} of 15 mM would cause a 9.3 mV error in the potentiometric value of the Cl$^-$ ISM, corresponding to an overestimate of a_{Cl} as 5.9 mM. In contrast, the high Cl-selectivity we observed for an MC3-ISM, $\log_{10}(K^{pot}_{Cl,HCO3}) = -2$, would result in only a 0.9 mV error with an estimated value of $a_{Cl} = 4.14$ mM. Insensitivity to HCO_3^- (Fig. 4) is also important because intracellular pH often changes or is intentionally manipulated during a study. The accompanying fluctuations of intracellular a_{HCO3} would render the potentiometric response uninterpretable for a poorly selective Cl$^-$ ISM. Sensitivity to pH is also a limitation for genetically encoded Cl sensors based on YFP variants, which has led to the development of ratiometric dual-sensor fluorescent proteins (ClopHensor) to monitor both [Cl] and pH simultaneously[43].

Another selectivity-based limitation of earlier Cl$^-$ ISMs was interference from drugs used to block Cl$^-$ channels (e.g. 9-ACA) or to inhibit Cl$^-$ exchangers and cotransporters (e.g. SITS, bumetanide, furosemide). These compounds are often used in studies of Cl transport, where drug-dependent changes in extracellular and intracellular Cl$^-$ activity are measured with ISMs. These inhibitors have high lipid solubility and are anions at physiologic pH, and so not surprisingly, substantial anion interference occurs for ISMs using poorly selective ionophores such as Corning 477413. For example, furosemide at 100 μM caused nonlinear potentiometric responses for $a_{Cl} \leq 30$ mM, with a corresponding selectivity coefficient of $K^{Pot}_{Cl,Fu} = 157$[35]. We tested three drugs that inhibit Cl$^-$ transport: furosemide, bumetanide, and 9-AC. In furosemide, we detected mild deviations from linear Nernstian behavior for MC3-ISM electrodes when $a_{Cl} \leq 1.6$ which is 20-fold lower than for Corning 477413 (Fig. 6C,F). In contrast, the potentiometric response of the MC3-ISM over the entire range of test solutions ([Cl] from 1 to 100 mM) was not affected by 20 μM bumetanide (Fig. 6B), which is ten times the IC$_{50}$ to inhibit the Na-K-2Cl 1 cotransporter. For the ClC-1 channel blocker, we detectable interference in 200 μM 9-ACA when [Cl] <10 mM (Fig. 6A). Studies in skeletal muscle typically use 100 μM 9-ACA, and at this lower concentration we detected a change in the MC3-ISM response only for [Cl] <2.5 mM. Overall, the MC3-ISM is highly selective for Cl with a linear Nernstian response over the biologically meaningful operating range of 1 to 100 mM, with no interference from endogenous anions (10 mM HCO_3^-, PO_4^-, or lactate) or bumetanide and very modest effects in high-dose 9-ACA well above the IC$_{50}$.

Finally, we demonstrate that the MC3-ISM reliably measures a_{Cl} in a biological context, the intracellular activity in an isolated skeletal muscle fiber (Fig. 7). The response to an external Cl-free challenge is a stringent test of the MC3-ISM because the resulting decrease of intracellular a_{Cl} would reveal effects from interfering intracellular anions or other sources of distortion as an attenuation of the change in the potentiometric signal. The response in Fig. 7 clearly shows a large response for $V_{Cl} = -(V_{MC3-ISM} - V_{ref})$, corresponding to a decrease of intracellular a_{Cl} to less than 2 mM. The record in Fig. 7 also shows the high quality of the signal-to-noise for measuring intracellular a_{Cl}, as well as the stability of the response with no significant drift and a return to the same baseline when external Cl is restored 10 minutes later. Measurement of intracellular a_{Cl} is also of great interest in studies of the nervous system because the Nernst potential for Cl$^-$ determines the postsynaptic response to activation of glycine and GABA$_A$ receptors. Moreover, intracellular Cl$^-$ varies over time, ranging from 3 to 20 mM or higher. Neuronal intracellular Cl$^-$ is high in the immature brain, in part due to activity of NKCC1 that promotes Cl$^-$ influx, and so receptor activation elicits post-synaptic depolarization (i.e. excitation). With development, NKCC1 decreases and is replaced by KCC that promotes Cl$^-$ efflux[3,44,45]. The reduced intracellular Cl$^-$ shifts the Nernst potential for Cl$^-$ below the resting potential and receptor activation now produces hyperpolarization (inhibition). Derangements of the Cl$^-$ gradient in the neurons have been implicated in epilepsy[46] and in anomalous regulation of cell volume that drives proliferation and migration of gliomas[47]. The MC3-ISM offers an improved approach for measuring somatic a_{Cl} for the determination of basal levels and changes that may occur over seconds to minutes – for example in response to inhibition of specific transporters. Of course alternative methods, such as dye fluorescence lifetime[9] or genetically encoded Cl-sensors[10], are required to measure local a_{Cl} changes within diffusion-restricted spaces in out in the dendrites or for fast transients less than 3 sec.

References

1. Shcheynikov, N. *et al.* Intracellular Cl⁻ as a signaling ion that potently regulates Na$^+$/HCO$_3^-$ transporters. *Proc Natl Acad Sci USA* **112**, E329–337, https://doi.org/10.1073/pnas.1415673112 (2015).
2. Stauber, T., Weinert, S. & Jentsch, T. J. Cell biology and physiology of CLC chloride channels and transporters. *Comprehensive Physiology* **2**, 1701–1744, https://doi.org/10.1002/cphy.c110038 (2012).
3. Rivera, C. *et al.* The K$^+$/Cl$^-$ co-transporter KCC2 renders GABA hyperpolarizing during neuronal maturation. *Nature* **397**, 251–255, https://doi.org/10.1038/16697 (1999).
4. Hodgkin, A. L. & Horowitcz, P. The influence of potassium and chloride on the membrane potential of single muscle fibres. *J. Physiol.* **148**, 127–160 (1959).
5. Pedersen, T. H., de Paoli, F. & Nielsen, O. B. Increased excitability of acidified skeletal muscle: role of chloride conductance. *J Gen Physiol* **125**, 237–246 (2005).
6. Mi, W., Wu, F., Quinonez, M., DiFranco, M. & Cannon, S. C. Recovery from acidosis is a robust trigger for loss of force in murine hypokalemic periodic paralysis. *J Gen Physiol* **151**, 555–566, https://doi.org/10.1085/jgp.201812231 (2019).
7. Wu, F., Mi, W. & Cannon, S. C. Bumetanide prevents transient decreases in muscle force in murine hypokalemic periodic paralysis. *Neurology* **80**, 1110–1116, https://doi.org/10.1212/WNL.0b013e3182886a0e (2013).
8. Tsien, R. Y. Intracellular measurements of ion activities. *Annu Rev Biophys Bioeng* **12**, 91–116, https://doi.org/10.1146/annurev.bb.12.060183.000515 (1983).
9. Gensch, T., Untiet, V., Franzen, A., Kovermann, P. & Fahlke, C. In *Advanced Time-Correlated Single Photon Counting Applications* (ed. Becker, W.) 189–211 (Springer International Publishing, 2015).
10. Arosio, D. & Ratto, G. M. Twenty years of fluorescence imaging of intracellular chloride. *Front Cell Neurosci* **8**, 258, https://doi.org/10.3389/fncel.2014.00258 (2014).
11. Standen, N. B. G., Gray, P. T. A. & Whitakwer, M. J. *Microelectrode techniques*, 137–167 (The Company of Biologists Limited, 1987).
12. Lee, S. K., Boron, W. F. & Parker, M. D. Monitoring ion activities in and around cells using ion-selective liquid-membrane microelectrodes. *Sensors (Basel)* **13**, 984–1003, https://doi.org/10.3390/s130100984 (2013).
13. Fedirko, N., Svichar, N. & Chesler, M. Fabrication and use of high-speed, concentric h$^+$- and Ca^{2+}-selective microelectrodes suitable for *in vitro* extracellular recording. *J Neurophysiol* **96**, 919–924, https://doi.org/10.1152/jn.00258.2006 (2006).
14. Messerli, M. A., Collis, L. P. & Smith, P. J. Ion trapping with fast-response ion-selective microelectrodes enhances detection of extracellular ion channel gradients. *Biophys J* **96**, 1597–1605, https://doi.org/10.1016/j.bpj.2008.11.025 (2009).
15. Alvarez-Leefmans, F. J., Giraldez, F. & Russell, J. M. In *Chloride CHannels and Carriers in Nerve, Muscle, and Glial Cells* (eds Alavarez-Leefmans, F. J. & Russell, J. M.) Ch. 1, 3–66 (Springer, 1990).
16. Davis, A. P., Sheppard, D. N. & Smith, B. D. Development of synthetic membrane transporters for anions. *Chem Soc Rev* **36**, 348–357, https://doi.org/10.1039/b512651g (2007).
17. Share, A. I. *et al.* Chloride anion transporters inhibit growth of methicillin-resistant Staphylococcus aureus (MRSA) *in vitro. Chem Commun (Camb)* **52**, 7560–7563, https://doi.org/10.1039/c6cc03645g (2016).
18. Shen, B., Li, X., Wang, F., Yao, X. & Yang, D. A synthetic chloride channel restores chloride conductance in human cystic fibrosis epithelial cells. *PLoS One* **7**, e34694, https://doi.org/10.1371/journal.pone.0034694 (2012).
19. Choi, Y. R., Chae, M. K., Kim, D., Lah, M. S. & Jeong, K. S. Synthetic chloride transporters with the binding mode observed in a ClC chloride channel. *Chem Commun (Camb)* **48**, 10346–10348, https://doi.org/10.1039/c2cc35743g (2012).
20. Li, H. *et al.* Efficient, non-toxic anion transport by synthetic carriers in cells and epithelia. *Nat Chem* **8**, 24–32, https://doi.org/10.1038/nchem.2384 (2016).
21. McNally, B. A. *et al.* Structure-activity relationships in cholapod anion carriers: enhanced transmembrane chloride transport through substituent tuning. *Chemistry* **14**, 9599–9606, https://doi.org/10.1002/chem.200801163 (2008).
22. Badr, I. H., Diaz, M., Hawthorne, M. F. & Bachas, L. G. Mercuracarborand "anti-crown ether"-based chloride-sensitive liquid/polymeric membrane electrodes. *Anal Chem* **71**, 1371–1377 (1999).
23. Yang, X., Zheng, Z., Knobler, C. B. & Hawthorne, M. F. "Anti-Crown" chemistry: Synthesis of [9]mercuracarborand-3 and the crystal structure of its acetonitrile complexes. *J. Am. Chem. Soc.* **115**, 193–195 (1993).
24. Parsons, R. *Handbook of electrochemical constant*, 20–28 (Butterworth, 1959).
25. Debye, P. & Hückel, E. The theory of electrolytes I. Lowering of freezing point and related phenomena. *Physikalische Zeitschrift* **24**, 185–206 (1923).
26. Woods, C. E., Novo, D., DiFranco, M. & Vergara, J. L. The action potential-evoked sarcoplasmic reticulum calcium release is impaired in mdx mouse muscle fibres. *J Physiol* **557**, 59–75 (2004).
27. Umezawa, Y., Buhlmann, P., Umezawa, J., Tohda, K. & Ameniya, S. Potentiometric selectivity coefficients of ion-selective electrodes. *Pure Applied Chemistry* **72**, 1851–2082 (2000).
28. Habela, C. W., Ernest, N. J., Swindall, A. F. & Sontheimer, H. Chloride accumulation drives volume dynamics underlying cell proliferation and migration. *J Neurophysiol* **101**, 750–757, https://doi.org/10.1152/jn.90840.2008 (2009).
29. Bolton, T. B. & Vaughan-Jones, R. D. Continuous direct measurement of intracellular chloride and pH in frog skeletal muscle. *J Physiol* **270**, 801–833 (1977).
30. Huser, M. *et al.* Transport properties of anion-selective membranes based on cobyrinates and metaloporphyrin complexes as ionophores. *Chimica Acta* **73**, 1481–1496 (1990).
31. Aickin, C. C., Betz, W. J. & Harris, G. L. Intracellular chloride and the mechanism for its accumulation in rat lumbrical muscle. *J Physiol* **411**, 437–455 (1989).
32. Vaughan-Jones, R. D. Non-passive chloride distribution in mammalian heart muscle: micro-electrode measurement of the intracellular chloride activity. *J Physiol* **295**, 83–109 (1979).
33. Khuri, R. N., Agulian, S. K. & Bogharian, K. K. Intracellular bicarbonate of skeletal muscle under different metabolic states. *Am J Physiol* **230**, 228–232 (1976).
34. Messerli, M. A., Kurtz, I. & Smith, P. J. Characterization of optimized Na$^+$ and Cl$^-$ liquid membranes for use with extracellular, self-referencing microelectrodes. *Anal Bioanal Chem* **390**, 1355–1359, https://doi.org/10.1007/s00216-007-1804-z (2008).
35. Chao, A. C. & Armstrong, W. M. Cl(−)-selective microelectrodes: sensitivity to anionic Cl$^-$ transport inhibitors. *Am J Physiol* **253**, C343–347, https://doi.org/10.1152/ajpcell.1987.253.2.C343 (1987).
36. Palade, P. T. & Barchi, R. L. On the inhibition of muscle membrane chloride conductance by aromatic carboxylic acids. *The Journal of general physiology* **69**, 879–896 (1977).
37. Glykys, J. *et al.* Local impermeant anions establish the neuronal chloride concentration. *Science* **343**, 670–675, https://doi.org/10.1126/science.1245423 (2014).
38. Kondo, Y., Buhrer, T., Seiler, K., Fromter, E. & Simon, W. A new double-barrelled, ionophore-based microelectrode for chloride ions. *Pflugers Arch* **414**, 663–668 (1989).
39. Rothmaier, M. & Simon, W. Chloride-selective electrodes based on mercury organic compounds as neutral carriers. *Analytica Chimica Acta* **271**, 135–141 (1993).
40. Spokoyny, A. M. *et al.* A coordination chemistry dichotomy for icosahedral carborane-based ligands. *Nat Chem* **3**, 590–596, https://doi.org/10.1038/nchem.1088 (2011).
41. Yruegas, S., Axtell, J. C., Kirlikovali, K. O., Spokoyny, A. M. & Martin, C. D. Synthesis of 9-borafluorene analogues featuring a three-dimensional 1,1′-bis(o-carborane) backbone. *Chem Commun (Camb)* **55**, 2892–2895, https://doi.org/10.1039/c8cc10087j (2019).

42. Baumgarten, C. M. An improved liquid ion exchanger for chloride ion-selective microelectrodes. *Am J Physiol* **241**, C258–263, https://doi.org/10.1152/ajpcell.1981.241.5.C258 (1981).
43. Arosio, D. *et al*. Simultaneous intracellular chloride and pH measurements using a GFP-based sensor. *Nat Methods* **7**, 516–518, https://doi.org/10.1038/nmeth.1471 (2010).
44. Kakazu, Y., Akaike, N., Komiyama, S. & Nabekura, J. Regulation of intracellular chloride by cotransporters in developing lateral superior olive neurons. *J Neurosci* **19**, 2843–2851 (1999).
45. Kahle, K. T. *et al*. Roles of the cation-chloride cotransporters in neurological disease. *Nature clinical practice* **4**, 490–503, https://doi.org/10.1038/ncpneuro0883 (2008).
46. Glykys, J. *et al*. Chloride Dysregulation, Seizures, and Cerebral Edema: A Relationship with Therapeutic Potential. *Trends Neurosci* **40**, 276–294, https://doi.org/10.1016/j.tins.2017.03.006 (2017).
47. Ransom, C. B., O'Neal, J. T. & Sontheimer, H. Volume-activated chloride currents contribute to the resting conductance and invasive migration of human glioma cells. *J Neurosci* **21**, 7674–7683 (2001).

Acknowledgements

Author contributions

The experimental design was conceived by M.D., S.C. and A.S. MC3 was synthesized by R.D. Measurement of ISM responses were performed by M.Q. and M.D. The paper was written by M.D., S.C. and A.S. All authors reviewed the final manuscript and approved the content.

Competing interests

The authors declare no competing interests.

Additional information

Correspondence and requests for materials should be addressed to S.C.C.

Reprints and permissions information is available at www.nature.com/reprints.

Publisher's note Springer Nature remains neutral with regard to jurisdictional claims in published maps and institutional affiliations.